THE ASTROPHYSICAL JOURNAL, 472:73–82, 1996 November 20

HUBBLE SPACE TELESCOPE OBSERVATIONS OF QSO ABSORPTION LINES ASSOCIATED WITH STARBURST GALAXY OUTFLOWS[1]

COLIN A. NORMAN,[2,3] DAVID V. BOWEN,[3,4] TIM HECKMAN,[2] CHRIS BLADES,[3] AND LAURA DANLY[3]
Received 1996 March 15; accepted 1996 May 10

ABSTRACT

In order to study the physical state of outflows from starburst galaxies, we have been obtaining spectra of QSOs located behind possible starburst outflows and searching for UV absorption by low-ionization gas. We have detected strong and probably complex Mg II, Mg I, and Fe II absorption arising from gas in the outer envelope of the starburst galaxy NGC 520 at a distance from the galactic nucleus of 24 h^{-1} kpc and possible weak Mg II absorption at a distance of 52 h^{-1} kpc. The detection of absorption at these distances is consistent with the idea that the size of gaseous envelopes around starburst galaxies is greatly enhanced from outflows of gas from the galaxies' nuclei, but it is also possible that the absorption arises from tidally disrupted gas associated with the interactions between NGC 520 and a dwarf galaxy companion. In the former case, the data would be consistent with starburst outflows generating the QSO absorption lines observed in extended halos at high redshift. In the latter case, the data is consistent with the low-redshift Mg II absorbers being associated with tidal debris.

We have also searched for Mg II absorption along two sight lines toward NGC 253, both at a distance of 44 kpc from the galaxy. Complex structure is seen, which may arise in gas associated with NGC 253. However, any absorption at the systemic velocity of NGC 253 is expected to be close to local Galactic absorption, and indeed the Mg II lines seen toward Q0042−2450 from the Milky Way are resolved and asymmetric. However, the sight lines to this QSO pass close to the Magellanic Stream, and we suggest that, with the current data, an equally likely possibility is that the additional absorption may arise in low column density gas associated with the Stream.

Further searches for high-ionization absorption lines (such as C IV and N V) from starburst outflows in NGC 253 and other galaxies may well be successful.

Subject headings: galaxies: halos — galaxies: starburst — quasars: absorption lines — ultraviolet: galaxies

1. INTRODUCTION

The detection of metal line absorption in QSO spectra at redshifts of $\sim$0.2–4 is widely attributed to the presence of foreground galaxies. In particular, galaxies that are apparently responsible for Mg II absorption at intermediate redshifts have been found at impact parameters of $\leq 40\ h^{-1}$ kpc from QSO sight lines in a large number of fields (e.g., Bergeron 1986; Steidel 1993; Steidel, Dickinson, & Persson 1994), and this value for the impact parameter is close to that implied by the frequency of Mg II detections in QSO absorption-line surveys. On the other hand, there remains considerable discussion about the nature of the proposed absorbing galaxies (e.g., spirals or irregular galaxies or starbursts), as well as on the exact location of the absorbing clouds (e.g., in extended halos or disks or in possible tidal material).

In an effort to find the present-day analogs of the higher redshift galaxies responsible for absorption in QSOs, we have been using the *Hubble Space Telescope* (*HST*) to study QSOs behind nearby intervening galaxies. There are several advantages of probing present-day galaxies: first, searches for Mg II lines are conducted without a priori knowledge of an absorption system, therefore all galaxies are tested for the existence of absorbing halos; second, the morphology and environment of a low-redshift galaxy is easily discerned; and third, as intermediate-redshift absorbing galaxies become better understood, identification of low-redshift absorbers will enable us to trace the evolution of galaxies that is now being seen directly with *HST*.

Accordingly, Bowen, Blades, & Pettini (1995, hereafter BBP) have published results from their study of Mg II absorption from 17 low-redshift galaxies that are of diverse morphological type and that reside in different environments. Mg II was found relatively rarely and only for small values of the impact parameter. Detected galaxies were predominantly spirals. As mentioned, however, there is evidence of a population of starburst galaxies at earlier epochs, and so we have been anxious to extend our present epoch absorption-line searches to this type of system. In this paper, we report our first results from an examination of four QSOs behind two starburst galaxies.

Starburst galaxies are known to pump prodigious amounts of mass, energy, and momentum into their circumgalactic halos and the surrounding intergalactic medium (see Heckman, Armus, & Miley 1990). These flows can be seen in warm gas (via optical-line emission), in hot gas (via X-ray emission), and in relativistic plasma (via radio synchrotron emission). The flows are usually of a bipolar morphology and contain filamentary structure seen in optical emission lines embedded in a hot X-ray emitting gas. The flow velocities range from 300 to 1000 km s^{-1}. The pressure

[1] Based on observations obtained with the NASA/ESA *Hubble Space Telescope*, collected at the Space Telescope Science Institute, which is operated by the Association of Universities for Research in Astronomy, Inc., under contract with the National Aeronautics and Space Administration, NAS 5-26555.

[2] Johns Hopkins University, Charles and 34th Street, Bloomberg Center, Baltimore, MD 21218.

[3] Space Telescope Science Institute, 3700 San Martin Drive, Baltimore, MD 21218.

[4] Royal Observatory, Blackford Hill, Edinburgh EH9 3HJ, Scotland, UK.

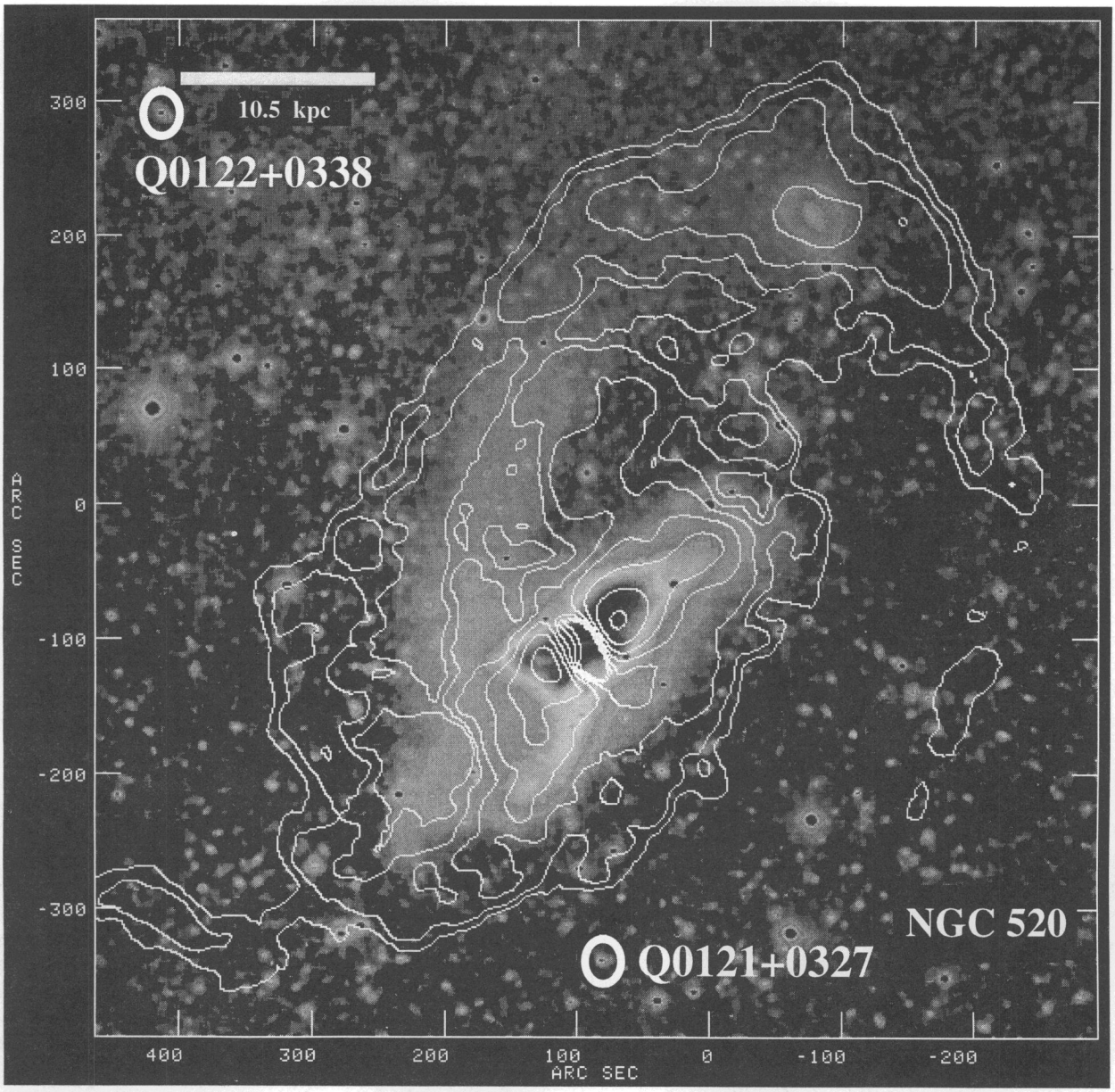

FIG. 1.—Contour map of 21 cm emission from NGC 520 superimposed on an optical image of the galaxy (taken from Hibbard & van Gorkom 1996). Lowest H I contour shown corresponds to a column density of 2×10^{19} cm^{-2}. Positions of the target QSOs are indicated by white circles.

is inferred to fall off with radial distance from the galaxy center roughly as r^{-2}.

The physics of these flows is fascinating. The most plausible explanation of their origin is that they are driven by a continuous energy and momentum input from supernovae explosions generated as massive stars formed in the burst evolve and explode. The star formation rates are of order 10–100 $M_\odot$ yr^{-1}, with corresponding supernovae rates of 0.1–1 yr^{-1}. Gas heated by the continuously occurring supernovae expands out of the galactic disk, merging into the massive bipolar galactic outflow. The focusing mechanism of the outflow is probably caused by the presence of the steep vertical density gradient in the galactic disk.

Clearly such outflows can be very important for the heavy-element enrichment process for galactic halos, as well as the surrounding intracluster and intergalactic gas. This may have important ramifications for the origin of metal-rich absorption lines seen in QSO spectra. Furthermore, the overall flow of mass, energy, and momentum from disk to halo is an important parameter in determining the nature of a galaxy's interstellar medium (Norman & Ikeuchi 1989). Thus, the flows may be fundamental to our understanding of the problems of chemical enrichment of the halo and the disk, as well as the redistribution of mass in the disk-halo system as a function of galactocentric distance (both in and normal to the galactic plane). It is quite possible that catastrophic events—such as these starburst episodes—can totally dominate the evolution of galaxies.

Our current *HST* program constitutes part of a detailed study of the physical state of these outflows. Absorption lines detected from the outflowing gas can provide important information on the extent of the outflow, its filling factor, ionization state, geometry, and kinematics. They will also provide an interesting comparison with similar data obtained from our own halo and nearby normal galaxies, and they may shed important information on the origin of

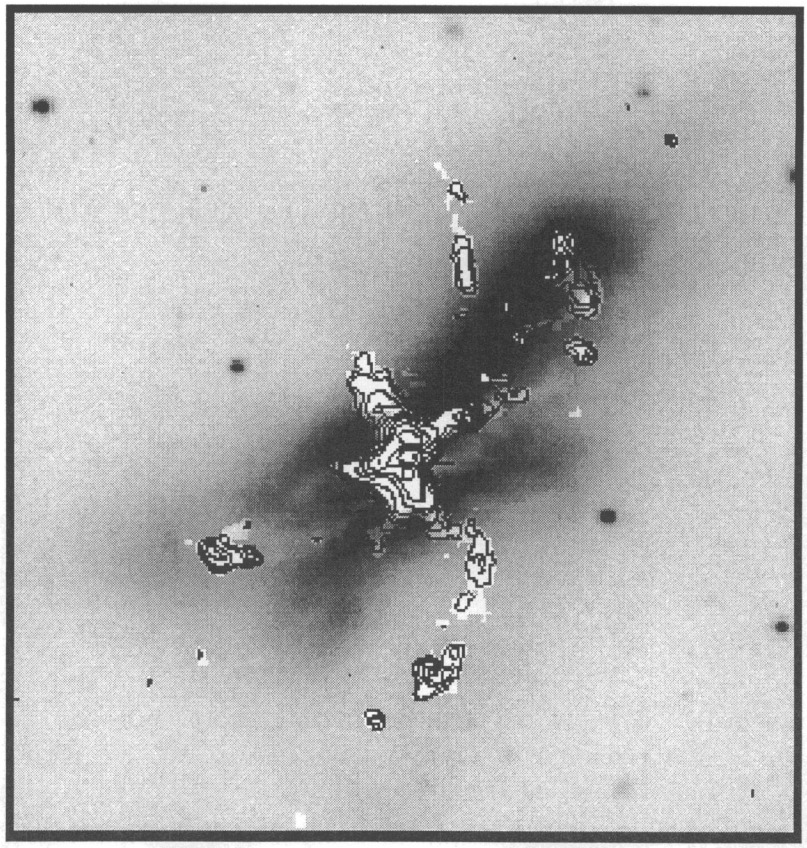

FIG. 2.—Continuum subtracted Hα + [N II] contours superimposed on an R-band image of NGC 520 (Hibbard & van Gorkom 1996). Note the filaments of Hα emission extending about 0.5 on either side of the starburst along the galaxy's minor axis.

complex absorption systems observed in the spectra of high-redshift QSOs. Such observations can provide unique information on the physical state of these complex galactic processes, information that cannot be determined by any other method.

In this paper, we have searched for absorption lines toward two starburst galaxies, NGC 520 and NGC 253. NGC 520 is an IR bright galaxy with a highly disturbed but flattened optical morphology (Fig. 1), interacting with a dwarf galaxy to the northwest. Its far-IR luminosity is similar to that of NGC 253 and M82. It has a pronounced central concentration of molecular gas and exhibits strong optical-line emission from an ensemble of giant H II regions. The Hα image (Fig. 2; Hibbard & van Gorkom 1996) and an archival *ROSAT* Position Sensitive Proportional Counter (PSPC) image (Fig. 3) show filamentary structures extending far out along the galaxy's minor axis, suggesting that an outflow of warm and hot gas is occurring.

The second galaxy, NGC 253 (see Pocock, Blades, & Penston 1984; Monk et al. 1986), is (along with M82) the prototype of the class of starburst galaxies. It has a far-IR luminosity of about $3 \times 10^{10}\ L_{\odot}$, most of which is produced in a dense molecular disk with a diameter of several hundred pc. The estimated star formation rate is about 10 $M_{\odot}\ \mathrm{yr}^{-1}$. Hα images and long-slit spectra show that there is a region of outflowing gas to the southeast of the nucleus along the disk minor axis, coinciding with a thermal X-ray nebula (McCarthy, Heckman, & van Breugel 1987; Heckman et al. 1990). The inferred outflow velocity is 300–400 km s^{-1} for the optical emission-line gas, which appears to reside in the walls of a conelike structure filled with the hot X-ray gas. The optical manifestation of the outflow can only be traced out to a distance of a few kpc before the emission becomes undetectably faint. In contrast, deep *ROSAT* PSPC images (Pietsch 1993) allow the X-ray emission to be traced out to a radius of about 15 kpc on both sides of the galactic disk.

In § 2, we give the observations and data reduction; in § 3, we discuss the results; and in § 4, we present our discussion and summary.

2. OBSERVATIONS & DATA REDUCTION

2.1. *Selection of Targets*

We have observed four QSOs located behind NGC 253 and NGC 520. The two targets toward NGC 253 (Q0048−2608 and Q0042−2450) were discovered by Pocock et al. (1984). The targets were selected because their sight lines pass perpendicular to the major axis of the highly inclined galaxy; these lines of sight may therefore intercept any gaseous outflows associated with the starburst phenomenon. The QSOs behind NGC 520 were taken from Arp & Duhalde (1985). The QSOs were originally labeled as objects 40 and 48 in Arp & Duhalde, but they are designated herein as Q0122+0338 and Q0121+0327, respectively. These QSOs are listed in Table 1, along with their original aliases (col. [2]), their *V*-band magnitude (taken from Véron-Cetty & Véron 1993; col. [3]), and their emission redshifts (col. [4]).

We attempted to observe Q0958+5557, which was selected because of its proximity to NGC 3079. This QSO is one of three UV-excess QSOs near NGC 3079 and Mrk 131

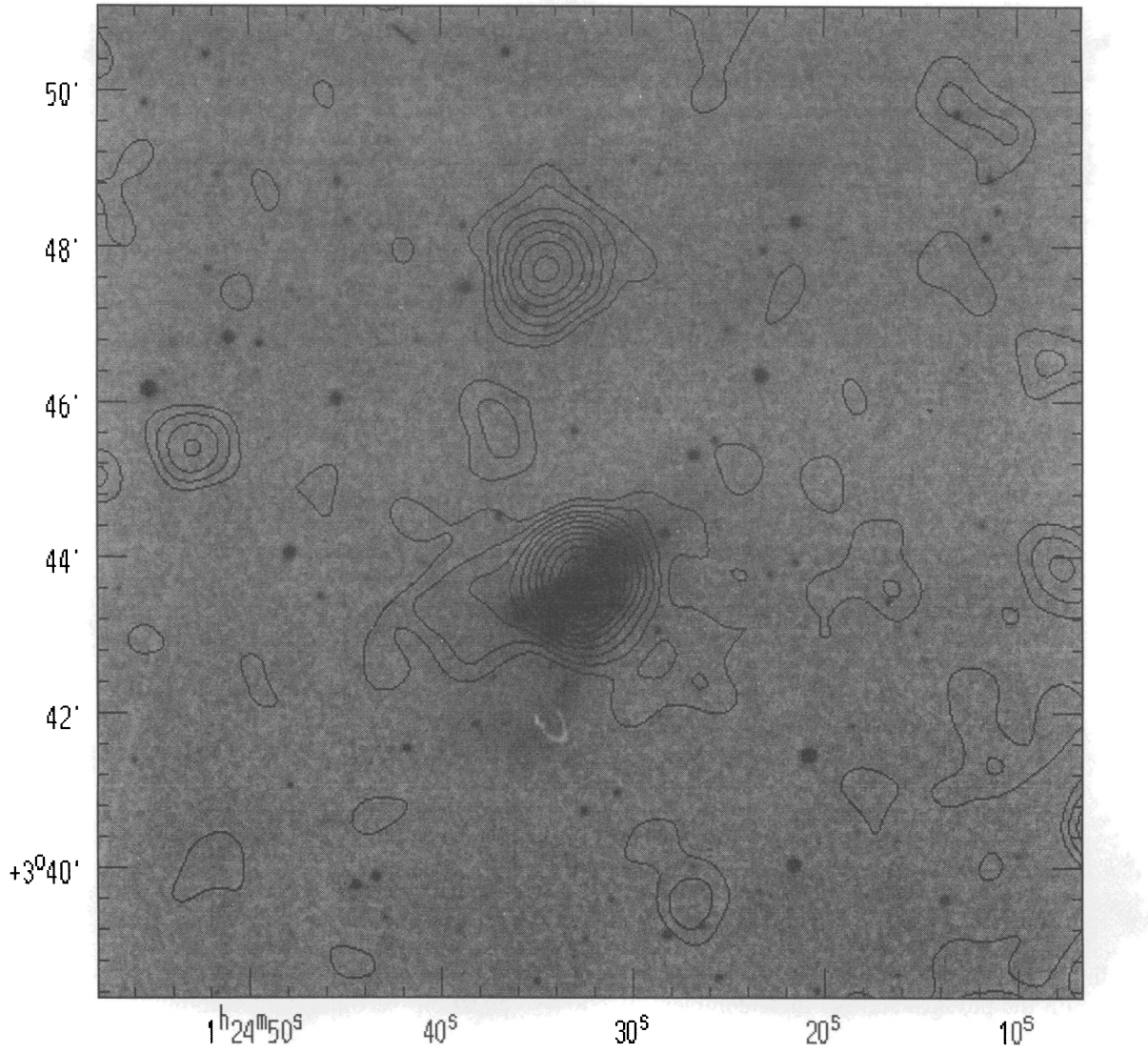

FIG. 3.—Archival *ROSAT* PSPC image of the X-ray emission in NGC 520. Note the bright central source coincident with the starburst and the plumes of emission extending about 2′ to the east and southwest—roughly along the galaxy's minor axis.

observed by Arp (1981), and it was originally designated as "UB4." However, our FOS spectrum of Q0958+5557 was found to have a significantly lower flux than expected, owing to the presence of a Lyman limit system at $z = 1.1327$ (Womble, Junkkarinen, & Burbridge 1992). This spectrum, therefore, had too low a signal-to-noise ratio to study any absorption from the outflow of NGC 3079, and this sight line is not discussed further.

2.2. *Reduction of FOS Data*

The journal of observations is given in Table 1, which lists the date of the observation, the grating and aperture used, the exposure time, and the *HST* archive root name of the observations. The majority of the data were taken with the G270H grating and the red FOS detector in order to search for Mg II λλ2796, 2803, Mg I λ2852, and the Fe II

TABLE 1

JOURNAL OF FOS OBSERVATIONS

Target	Alias	V	z_e	Date	Grating	Aperture	Exposure Time (s)	root[a]
Q0958+5557.....	UB4	17.4	1.154	1992 Apr 27	G130H	0.25 × 2.0	14316	y0x1010
Q0122+0338.....	N520.40	17.7	1.205	1993 Sep 09	G270H	0.25 × 2.0	5760	y1by040
				1993 Nov 22	G270H	0.25 × 2.0	5760	y1by540
Q0042−2450.....	...	17.4	0.807	1995 Jun 30	G270H	0.3	4680	y2nl010
Q0048−2608.....	...	18.1	2.249	1995 Jul 02	G270H	0.3	6480	y2nl020
Q0121+0327.....	N520.48	18.5	0.336	1995 Jul 01	G270H	0.3	12600	y2nl030

[a] *HST* archive data set filename.

lines that lie redward of 2200 Å. Only Q0958+5557 was observed with the G130H and blue detector in order to search for high-ionization absorption lines from NGC 3079, such as C IV, Si IV, and N V. All targets were acquired using a four-step acquisition and peak-up sequence, except Q0958+5557, which stepped from the 4.3 aperture straight to the 0.25 × 2.0 slit.

The spectra were reduced using standard pipeline software. Individual data sets containing data taken over different exposure times were weighted by their measured signal-to-noise ratios and then co-added. Data were reduced to vacuum wavelengths and a heliocentric rest frame and were resampled to a linear wavelength scale with bin sizes equal to the original dispersion (0.51 Å pixel^{-1} for the G270H data).

To improve the wavelength calibration of the G270H data, we compared the velocity of the absorption by Mg II absorbing gas in our own Milky Way with the velocity of the bulk H I gas observed from 21 cm emission measurements. The H I spectra were taken from the Leiden/Dwingeloo 21 cm H I survey (Hartmann 1994), along the lines of sight toward NGC 520 and NGC 253. Implicit in this method is the assumption that the bulk of the Mg II absorption arises in the same gas (or at least at the same velocity) as the H I gas. Mg II arises in both neutral and ionized gas, but the velocity difference between the centroid of the absorption line arising from such a mixture of species, as well as the the centroid of the H I emission, is negligible compared to the errors in the zero point of the FOS wavelength calibration. Offsets of +2.3, +0.5, and +2.4 Å were required to bring the velocities of the local Mg II absorption lines to the H I velocities in the spectra of Q0042−2450, Q0122+0338, and Q0121+0327, respectively. No measurement of the wavelength of local absorption toward Q0048−2608 could be made because of the low signal-to-noise ratio of the spectrum; thus, no correction was made in that case.

Measurements of line positions and equivalent widths, W, were made on the original quarter-stepped data measured over 9 pixels, approximately twice the FWHM of the FOS line spread function, for most of the data sets. Q0122+0338 was observed before the implementation of COSTAR, and for these data, equivalent widths were measured over 13 pixels. The error arrays generated by the pipeline wavelength calibration do not include the contribution from the background or from other sources such as scattered light. Hence, objects with low count rates have error arrays that cannot be used to measure equivalent width limits, $\sigma(W)$. Instead, $\sigma(W)$ is estimated from $\sigma_c\sqrt{N}\,\delta\lambda$, where σ_c is the rms noise in the continuum at the wavelength of interest, $\delta\lambda$ is the dispersion (Å pixel^{-1}) and N is the number of pixels over which the line is measured.

3. RESULTS

3.1. *NGC 253, Q0042−2450, Q0048−2608*

Table 2 summarizes the pertinent information on NGC 253 and lists the separation of the QSOs from the galaxy on the plane of the sky. Q0042−2450 lies $\rho = 60.'1$ from the center of NGC 253, in the northwest quadrant of the galaxy (see Pocock et al. 1984; Monk et al. 1986). We have adopted a distance to the galaxy of $D = 2.58$ Mpc from Puche & Carignan (1988), which means that the QSO sight line passes through the halo of NGC 253 at a distance of $s = 44.1$ kpc. Q0048−2608 lies almost exactly opposite to Q0042−2450 in the southeast quadrant of NGC 253, $59.'9$ from the galaxy, or $s = 44.2$ kpc.

The normalized FOS spectra of both QSOs are shown in Figure 4. Since the velocity of NGC 253 is only 251 km s^{-1}, approximately the same as the resolution of the FOS, absorption from NGC 253 at its systemic velocity will only just be resolvable from local, Galactic absorption lines. The spectrum of Q0048−2608 is of low signal-to-noise ratio and is barely adequate to reveal the presence of Mg II absorption from NGC 253. Therefore, we do not discuss it further. Toward Q0042−2450, Mg II absorption from the Milky Way is resolved and shows some asymmetry in the blue wing of the absorption lines, which suggests that additional, weaker absorption may be present—as much as 200 km s^{-1} different from the bulk of the Galactic absorption (although this is impossible to quantify at the resolution of the FOS). Since absorption arising in outflowing gas from NGC 253 need not be at the systemic velocity of the galaxy, the shape of the absorption lines raises the possibility that this could be evidence for outflowing absorbing gas from NGC 253.

It is also possible that the additional absorption seen on the blue wing of the local Mg II λ2803 line at 2800.0 Å could be weak Mg II λ2796 absorption arising from gas associated with NGC 253 at a velocity of 390 km s^{-1}. However, the lack of any corresponding Mg II λ2803 absorption in a region of the spectrum clear of any lines makes it more likely that the feature at 2800 Å is merely a deviation from the moderate signal-to-noise data on the asymmetric profile of the local Mg II λ2803 line.

The evidence of complicated structure in the Mg II

TABLE 2

STARBURST GALAXIES PROBED BY QSOs

GALAXY PARAMETERS								QSO GALAXY SEPARATIONS			
Galaxy (1)	Type (2)	V_{gal} (km s^{-1}) (3)	D (Mpc) (4)	m_B (5)	M (6)	D_0 (arcmin) (7)	QSO PROBE (8)	ρ (arcmins) (9)	s (kpc) (10)	ρ' (h^{-1} kpc) (11)	$2\rho/D_0$ (12)
NGC 253.....	SAB(s)c	251	2.58	7.5	−19.6	27.6	Q0042−2450	60.1	44.1	...	4.4
							Q0048−2608	51.9	44.2	...	4.4
NGC 520.....	S pec	2266	20.8	11.8	−19.8	4.5	Q0122+0338	8.50	51.6	55.6	3.8
							Q0121+0327	3.85	23.9	25.7	1.8

NOTES.—Col (3) heliocentric velocity of galaxy. Col. (4) distance to galaxy, from Puche & Carignan 1988 (NGC 253) or Schoniger & Sofue 1994 (NGC 520). Cols. (5) and (7) face-on blue magnitude and optical diameter of galaxy, taken from RC3. Col. (6) absolute magnitude, from m_B and D. Col. (9) angular separation between QSO sight line and galaxy. Col (10) distance QSO sight line passes from center of galaxy, $s = 1000\,D\tan(\rho/60)$. Col. (11) distance QSO sight line passes from center of galaxy, derived from ρ assuming a Hubble Flow.

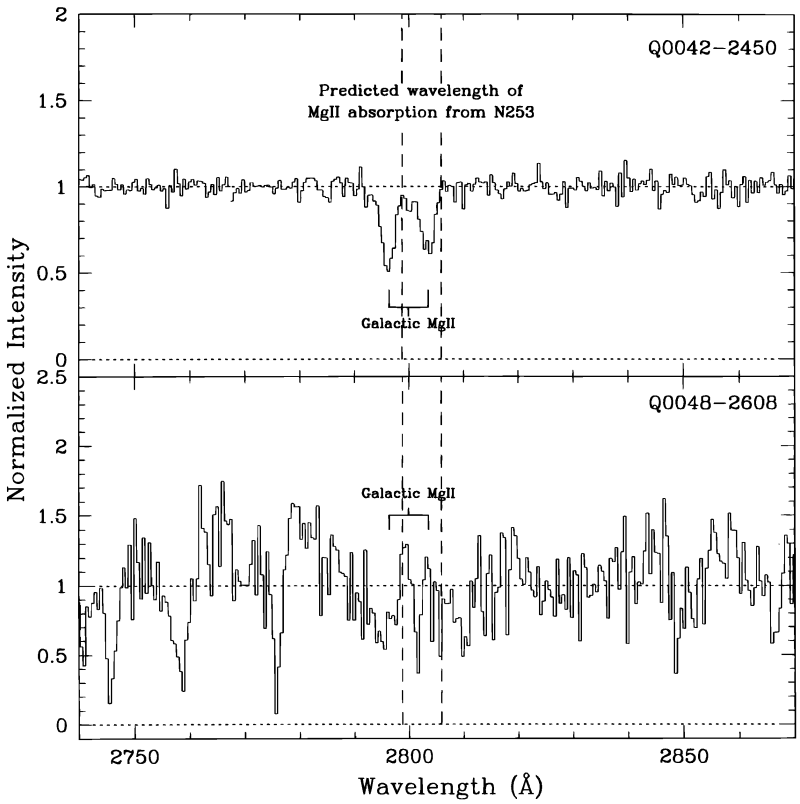

FIG. 4.—Normalized FOS spectra for two QSOs behind NGC 253, both lying 44 kpc from the galaxy. Mg II absorption from the Milky Way is indicated, and vertical dashed lines show the wavelength at which Mg II absorption is expected from NGC 520. Strong Mg II absorption is seen from the Milky Way toward Q0042−2450, but the lines are resolved, suggesting additional absorption extending to negative velocities. Although this could, in principle, be associated with gas 400–500 km s^{-1} different from the systemic velocity of NGC 253, it is more likely to arise from the Magellanic Stream, which passes only a few degrees away from the QSO sight line.

absorption lines may arise in gas associated with NGC 253, but with our current data we cannot be conclusive. Table 3 lists the equivalent width limits to the absorption lines that could have been detected, but it is calculated assuming that a line would have been resolved from the bulk of the local Milky Way absorption. For optically thin gas, an equivalent width limit given of 0.23 Å toward Q0042−2450 corresponds to a column density of $\log N(\mathrm{Mg\ II}) \leq 12.8$, although in principle a slightly stronger line could blend with Milky Way absorption lines and remain undetected. The mean gas density, n, in a starburst driven outflow is given by $n \sim (\dot{M}/\mu m_p V_w r^2)$, where $\dot{M}$ is the mass outflow in the wind, V_w is the wind velocity, and r is the galactocentric distance. For the nominal mass loss rate and wind velocity this yields $n \sim 10^{-3}$ cm^{-3}, which, in principle, is detectable by these observations. In realistic outflows, a multiphase structure develops and clumping of the gas into denser cloudlets occurs.

We note also that the sight line toward Q0042−2450 passes a few degrees away from the outer regions of the Magellanic Stream, between complexes MS III and MS IV (see, e.g., Mathewson & Ford 1984). There is no evidence for weak emission in the 21 cm spectrum toward NGC 253, but this does not rule out Mg II absorption arising in H I gas, with a column density below that detectable with the Dwingeloo 25 m telescope or in clouds with much smaller angular dimensions than the beam size of the telescope. The velocity of the additional absorption is at a velocity less than 0 km s^{-1}. This is consistent with the velocity of H I gas, found by Mirabel, Cohen, & Davies (1979; their "region 5") in a region 8°–9° away from the QSO sight line, at ≈ -150 km s^{-1}. It also roughly agrees with the general

TABLE 3

EQUIVALENT WIDTH MEASUREMENTS TOWARD BACKGROUND QSOs

GALAXY	QSO	V_{abs} (km s^{-1})	EQUIVALENT WIDTHS[a] Mg II λ2796 (Å)	Mg II λ2803 (Å)	Mg I λ2852 (Å)	Fe II λ2600 (Å)	Fe II λ2586 (Å)	Fe II λ2382 (Å)	Fe II λ2374 (Å)	Fe II λ2344 (Å)
NGC 253.....	Q0042−2450	...	<0.23	<0.23	<0.23	<0.32	<0.32	<0.28	<0.28	<0.28
	Q0048−2608	...	<0.09	<0.9	<0.9	<0.9	<0.9	<1.8	<1.8	<1.8
NGC 520.....	Q0121+0327	2285	1.72 ± 0.13	1.38 ± 0.12	0.23 ± 0.12	0.61 ± 0.12	0.26 ± 0.12	0.42 ± 0.12	<0.46	<0.46
	Q0122+0338	2492	0.33 ± 0.12	<0.36	<0.42	<0.45	<0.45	<0.60	<0.60	<0.60

[a] Where limits are given, these limits are 3 σ.

velocity field of the Magellanic Stream; in the coordinate system defined by Wannier & Wrixon (1972), the position of Q0042−2450 is at $\theta \approx 20$ degrees, which would put Magellanic stream gas at a velocity of ≈ -100 km s^{-1}.

We consider it equally plausible then that the absorption arises from low column density gas associated with the Magellanic Stream. This would not be the first time Mg II absorption has been detected from the Magellanic Stream: absorption is also seen toward 3C 454.3 and PKS 2251+11 in FOS spectra taken by Savage et al. (1993), although this absorption was associated with detectable 21 cm emission at velocities less than -350 km s^{-1} and arises in gas well away from the sight line of Q0042−2450 [l, b(3C 454.3) = 86, −38; l, b(PKS 2251+11) = 83, −42].

3.2. *NGC 520, Q0121+0327 and Q0122+0338*

Basic information for NGC 520 is again listed in Table 2. The line of sight toward Q0122+0338 is 8.′50 from the center of NGC 520; adopting a distance of 20.8 Mpc to the galaxy (Schoniger & Sofue 1994) means this separation corresponds to $s = 51.6$ kpc. This value is similar to that obtained assuming that the velocity of NGC 520 is a cosmological recession, $\rho' = 51.6\ h^{-1}$ kpc ($h = H_0/100$, where H_0 is the Hubble constant, $q_0 = 0$). Q0121+0327 is closer, at a separation of 3.′95, which corresponds to $s = 23.9$ kpc or $\rho' = 25.7\ h^{-1}$ kpc.

As Figure 5 shows, strong Mg II absorption is seen toward Q0121+0327 at a velocity of 2285 km s^{-1}, close to that of NGC 520. The lines are resolved and have asymmetric line profiles, extended in the blue, which suggests a multicomponent structure to the lines. Equivalent widths for these lines are given in Table 3. The complex structure and the fact that the lines are saturated (as deduced from the doublet ratio) means that it is difficult to calculate reliable column densities. The lower limit to the column density, calculated assuming that the gas is optically thin, is log N(Mg II) > 13.7. Mg II is also seen, as are Fe II lines: equivalent widths for these lines are again listed in Table 3. A simultaneous fit of theoretical Voigt profiles to the three Fe II lines using XVOIGT (Mar 1994) gives N(Fe II) ≈ 14.0 (with a Doppler parameter of $b = 24$ km s^{-1}); presumably, however, the Fe II lines must share a similar complicated structure to that of the Mg II, which makes this column density highly uncertain.

The sight line toward Q0122+0338 passes twice as far by NGC 520 than Q0121+0327, but there is evidence for weak Mg II λ2796 absorption arising from the galaxy at a higher velocity of 2490 km s^{-1}. Although there is no corresponding Mg II λ2803 line, the feature is significant and probably real at the 2–3 σ level. If so, the column density is restricted to, approximately, log N(Mg II) ≤ 13.3 for $b \geq 8$ km s^{-1}. Column densities higher than this or Doppler parameters less than this would produce an observable Mg II λ2803 line; but again, these values are very uncertain when derived from the low-resolution data of the FOS.

3.3. *Q0122+0338: $z_a \sim z_e$ System*

There is an interesting absorption-line system at the redshift of the Q0122+0338, where lines of N V, O VI, and Si IV

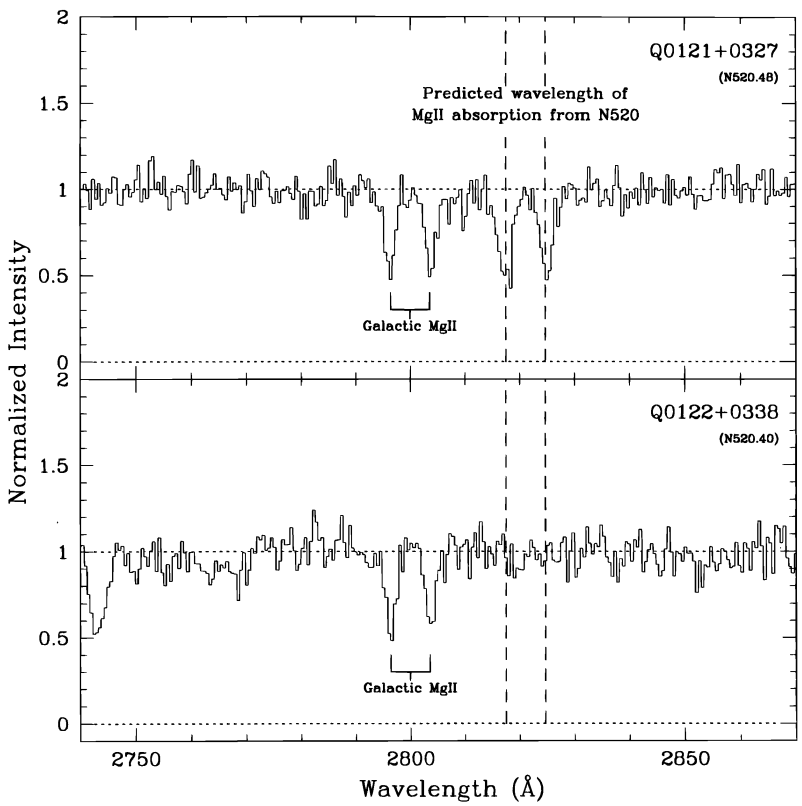

FIG. 5.—Normalized FOS spectra of two QSOs behind NGC 520. Mg II absorption from the Milky Way is indicated, and vertical dashed lines show the wavelength at which Mg II absorption is expected from NGC 520. Q0121+0327 (*top*) lies 24 kpc from the galaxy and shows strong Mg II absorption close to the systemic velocity of NGC 520. Absorption-line profiles are asymmetric, suggesting additional, weaker absorption at more negative velocities. Additional absorption would indeed be expected from the tidally disrupted gas seen in 21 cm emission around NGC 520. Mg I and Fe II absorption lines are also detected (see Table 3). Weak absorption is also seen toward Q0122+0338 (*bottom*), at slightly higher velocities. Since the line of sight to the QSO passes 52 kpc away from the galaxy, absorption at these distances is a surprise. Strong line at 2743 Å is N V λ1242, associated with a $z = 1.2$ absorption-line system.

TABLE 4

HIGH-IONIZATION LINES AT $z = 1.207$ TOWARD Q0122+0338

Ion	λ_{obs} (Å)	z_{abs}	W (Å)	$\sigma(W)$ (Å)
Lyβ	2264.1	1.2081	2.44	0.22
O VI λ1031.....	2278.2	1.2077	3.12	0.22
O VI λ1037.....	2290.7	1.2076	2.31	0.21
Lyα	2683.2	1.2072	3.38	0.12
N V λ1238	2734.2	1.2071	1.78	0.14
N V λ1242	2743.2	1.2073	1.59	0.14
Si IV λ1393.....	3075.6	1.2067	0.89	0.15
Si IV λ1402.....	3096.2	1.2072	0.20	0.15

are evident. Measurements of line positions and equivalent widths are given in Table 4. Detection of $z_a \sim z_e$ systems are relatively rare. Presumably, the gas is associated with the environment of the QSO itself or with an associated galaxy, thus explaining the higher level of ionization in the absorption system. We shall discuss this system in detail in a subsequent paper.

3.4. *Galactic Absorption Lines*

Absorption from the halo of the Milky Way is typical of what is seen toward other lines of sight through the Galactic halo. Absorption equivalent widths of Mg II $\lambda\lambda$2796, 2802 between 1 and 1.5 Å fall right in the range of previous studies (Savage et al. 1993; BBP) and are just what would be expected from saturated Mg II lines with a velocity width of about 100–150 km s^{-1}. Galactic H I emission data in the QSOs sight lines (Hartmann 1996, private communication) show 21 cm emission widths of about 100 km s^{-1} toward NGC 520 and about 150 km s^{-1} toward NGC 253. The larger equivalent widths observed toward NGC 253 are consistent with the larger velocity width of the Milky Way halo gas and may likely be associated with the Magellanic Stream, as noted above.

Absorption from Mg I and Fe II are also seen in the spectra. The equivalent widths and their ratios compared to Mg II are also typical of the Milky Way halo gas (Savage et al. 1993). Mn II is also suggested. However, the spectra have too low a signal-to-noise ratio to permit a reliable measurement of these lines for the determination of column densities via a curve-of-growth analysis.

4. DISCUSSION

4.1. *Comparison with Other* Mg II *Absorbing Galaxies*

To understand whether the detection of absorption toward NGC 520 or the nondetection of absorption toward NGC 253 is unusual, we compare the sight lines studied with those from the low-redshift Mg II survey of BBP and the higher redshift sample of Steidel (1995).

Figure 6 reproduces the BBP plot of QSO line-of-sight separation, ρ', from an intervening galaxy, against their absolute magnitude, M_B. Galaxies that give rise to absorption are represented by filled symbols; galaxies that do not show Mg II absorption to some upper limit are represented by unfilled symbols. ρ' and M_B are ambiguous in this figure because eight galaxies have distances independent of H_0 (*squares*), while others are in units of h^{-1} kpc (*triangles*). A bar is drawn from the symbol representing one of the low-redshift galaxies to show where it would lie for $H_0 = 50$ km s^{-1} Mpc^{-1}. Lines are also drawn to represent ρ' versus M_B for $R/R^* = (L/L^*)^\beta$ for galaxies with radii R (equivalent to ρ'). The solid line describes the Holmberg relation for stellar radii, $\beta = 0.4$ (here a galaxy with magnitude $M = -19.5$ has an optical radius of 14 h^{-1} kpc). The dashed line represents the Mg II absorption cross section for intermediate-redshift absorbing galaxies, $\beta = 0.2$ and $R^*_{gas} = 35\ h^{-1}$ kpc for $M^* = -19.5$ (Steidel 1993).

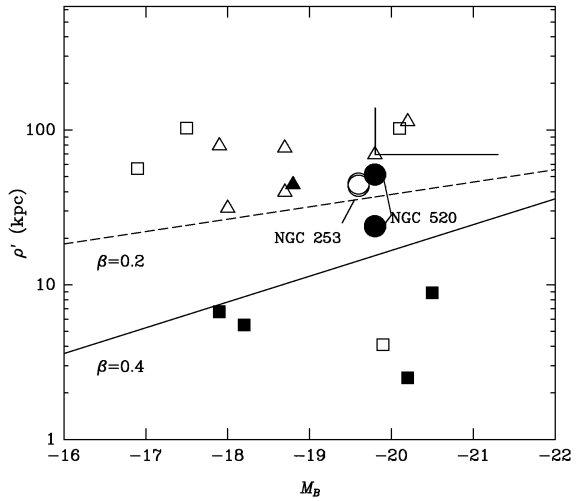

FIG. 6.—Plot of QSO line-of-sight separation, ρ', against absolute magnitude, M_B, of the low-redshift galaxies observed by BBP. Filled symbols represent detections of Mg II, while open symbols are upper limits. Lines are drawn to represent ρ vs. M_B for $R/R^* = (L/L^*)^\beta$ for galaxies with radii R (equivalent to ρ). Solid line describes the Holmberg relation for galaxy radii, $\beta = 0.4$ and the dashed line represents Mg II absorption cross section for intermediate-redshift absorbing galaxies $\beta = 0.2$ and $R^*_{gas} = 35\ h^{-1}$ kpc for $M^* = -19.5$ (Steidel 1993). Galaxies with distances independent of H_0 are represented by squares, while the others with distances in units of h^{-1} kpc are represented by triangles.

All the absorbing galaxies from the BBP survey, except those close to Q1543+489, lie beneath the $\beta = 0.2$ envelope and therefore are consistent with the cross section determined at intermediate redshift. G1543+4854 (*solid triangle* in Figs. 6 and 7) is unusual, having a luminosity about half that expected, and BBP suggested the detection of absorbing gas so far from the closest galaxy ($\rho' = 45\ h^{-1}$ kpc) was

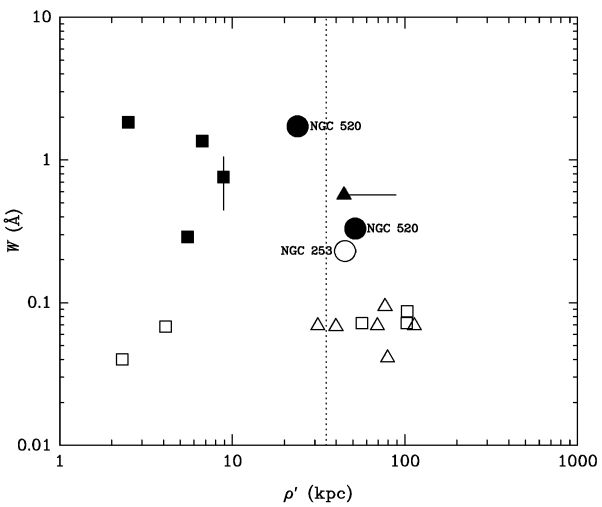

FIG. 7.—As for Fig. 6 but with equivalent width W vs. ρ. Sight line to Q0048−2608 has been excluded because of the low signal-to-noise ratio of the spectrum.

because the gas was distributed over large distances due to tidal disruptions from interactions between the galaxies close to the QSO sight line.

The possible detection of absorbing gas detected toward Q0122+0338 behind NGC 520 is therefore most interesting. Figure 6 shows that the absorption occurs outside the region found for the Mg II cross section of intermediate-redshift absorbing galaxies. The presence of gas at these distances is consistent with the idea that starburst outflows may give rise to extended absorption-line regions. An alternative possibility is that the 21 cm observations of the disrupted gas around NGC 520 suggest that it is the tidal disruption between the galaxy and the dwarf companion that distributes low column density gas more than 50 kpc from the galaxy (in the case of Q0122+0358). The detection of complex absorption from tidally disrupted gas around low-redshift galaxies is consistent with absorption seen, for example, toward M81 (Bowen et al. 1994) and the Large Magellanic Cloud (BBP). Simulations of the distribution of tidal debris produced in galaxy encounters (see Mihos 1995; Stanford & Balcells 1991) are consistent with the currently available data. Although both the distribution and kinematics of the gas for the two possibilities given above are quite distinct, we cannot, as yet, perform a clean observational test to clearly distinguish between them.

The $10 < \rho' < 30\ h^{-1}$ kpc, $-21 < M_B < -17$ region of parameter space not explored by BBP is sampled by the sight line toward Q0121+0327, which shows very strong Mg II absorption. Hence, the detection of Mg II lines at these impact parameters is consistent with that found from higher redshift galaxies and arises at distances beyond the conventional stellar radius of present-day galaxies. The asymmetric absorption-line profiles of the Mg II profiles can be understood as complex multicomponent absorption caused by outflows of gas from the starburst region of the galaxy.

Significantly, both sight lines pass beyond the last H I contour given by Hibbard & van Gorkom (1996), at a column of $N(\text{H I}) = 2 \times 10^{19}$ cm^{-2}. The absorbing gas toward Q0121+0327 produces strong Mg II absorption, as well as Mg I and Fe II; the absorption is reminiscent of that seen by our own Galaxy and suggests a large H I column density. Therefore, it may well be that absorption arises in small, dense cloudlets that are too small to be resolved by 21 cm maps, in the same way that high-velocity H I clouds could not be detected toward SN 1993J (Bowen et al. 1994), even though strong Mg II, Mg I, and Na I was detected in absorption. In contrast, the probable weak Mg II absorption seen toward Q0122+0338, which is unaccompanied by Mg I or Fe II lines, suggests absorption by a much more diffuse gas; for simple photoionization models of clouds bathed in an extragalactic UV background, Mg II disappears rapidly as the H I becomes optically thin at the Lyman limit (e.g., Bergeron & Stasinska 1986; Steidel & Sargent 1992), falling below 10^{12} cm^{-2} as the H I column density, N(H I), drops below 2×10^{17} cm^{-2}.

Figure 6 shows that the sight lines probing NGC 253 both pass beyond the Mg II cross section derived for the absorbing galaxies found at high redshift. Hence, the nondetection of Mg II absorption by NGC 253 at these distances is consistent with high-redshift sample of absorbing galaxies. However, this fact alone does not preclude the possibility that gas ejected from NGC 253 may extend large distances from the galaxy, since we would expect gas to be highly ionized. From *ROSAT* data on NGC 253 (Dahlem et al. 1996), we find a temperature of the hot gas at 10 kpc of 2×10^6 K. For adiabatic cooling in a free wind $T \propto r^{-4/3}$, where r is the Galactocentric distance. Thus, at 52 kpc we find a temperature of $\sim 2 \times 10^5$ K. Therefore, further searches for high-ionization absorption lines (such as C IV and N V) from starburst outflows in NGC 253 and other galaxies may well be successful. Note that if gas density becomes sufficiently low, then the recombination time exceeds the characteristic outflow time and the outflowing gas may be frozen into a higher ionization state, in which lines such as N V are not particularly abundant. However, in a realistic, multiphase outflowing gas the situation is more complex, and we expect that N V and associated species may be seen.

In conclusion, we have detected strong absorption caused by gas associated with the starburst galaxy NGC 520 in one background QSO (Q0121+0327) and possibly in a second target (Q0122+0338). We may also have detected absorption in NGC 253 using the background target Q0042−2450. Our results so far suggest that, indeed, starburst galaxies have extended envelopes, which most likely arise from nuclear outflows. However, to put this rather qualitative result on a quantitative footing, there are more observations that are needed: (1) for the targets that we have observed in this paper, we require high-resolution (*HST*-STIS) observations to resolve the velocity structure and to confirm the presence of the possible components; (2) we need to extend our observations to the higher ionization species, such as C IV and N V, as indicated above; and (3) additional starburst-QSO candidates need to be found and studied.

We thank our colleagues at the Space Telescope Science Institute and Johns Hopkins University for many interesting and useful discussions on this topic, and particularly Chris Mihos for valuable discussions on the distribution of tidal debris. We also thank Dap Hartmann for providing H I spectra from the Dwingeloo/Leiden 21 cm survey to help calibrate the FOS data, John Hibbard for permission to reproduce his images of NGC 520,0 and Kim Weaver for help with the archival *ROSAT* data on NGC 520. Support for this work was provided by NASA through grants GO 3676 and GO 2644 from the Space Telescope Science Institute, which is operated by the Association of Universities for Research in Astronomy, Inc., under NASA contract NAS 5-26555. Tim Heckman was supported in part by NASA grant NAGW-3138.

REFERENCES

Arp, H. 1981, ApJ, 250, 31
Arp, H., & Duhalde, O. 1985, PASP, 97, 1149
Bergeron, J. 1986, A&A, 155, L8
Bergeron, J., & Stasinska, G. 1986, A&A, 169, 1
Bowen, D. V., Blades, J. C., & Pettini, M. 1995, ApJ, 448, 634 (BBP)
Bowen, D. V., Roth, K. C., Blades, J. C., & Meyer, D. M. 1994, ApJ, 420, L71
Dahlem, et al. 1996, in preparation
Hartmann, D. 1994, Ph.D. thesis, Univ. Leiden
Heckman, T. M., Armus, L., & Miley, G. K. 1990, ApJS, 74, 833
Hibbard, J., & van Gorkom, J. H. 1996, AJ, 111, 655
Mar, D. P. 1994, Ph.D. thesis, Univ. Sydney
Mathewson, D. S., & Ford, V. L. 1984, in Structure and Evolution of the Magellanic Clouds, ed. S. van den Bergh & K. S. de Boer (Dordrecht: Kluwer), 125
McCarthy, P., Heckman, T. M., & van Breugel, W. 1987, AJ, 93, 264

Mihos, J. C. 1995, ApJ, 438, L75
Mirabel, I. F., Cohen, R. J., & Davies, R. D. 1979, MNRAS, 186, 433
Monk, A. S., Penston, M. V., Pettini, M., & Blades, J. C. 1986, MNRAS, 222, 787
Norman, C., & Ikeuchi, S. 1989, ApJ, 345, 372
Pietsch, J. 1993, in Panchromatic View of Galaxies—Their Evolutionary Puzzle, ed. G. Hensler (Paris: Frontieres), 137
Pocock, A. S., Blades, J. C., & Penston, M. V. 1984, MNRAS, 210, 373
Puche, D., & Carignan, C. 1988, AJ, 95, 1025
Savage, B. D., et al. 1993, ApJ, 413, 116
Schoniger, F., & Sofue, Y. 1994, A&A, 283, 21
Stanford, S. A., & Balcells, M. 1991, ApJ, 370, 118
Steidel, C. 1993, in The Environment and Evolution of Galaxies, ed. J. M. Shull & H. A. Thronson, Jr. (Dordrecht: Kluwer), 263
Steidel, C. 1995, in ESO Astrophysics Symp., QSO Absorption Lines, ed. G. Meylan (Berlin: Springer), 139
Steidel, C., Dickinson, M., & Persson, E. 1994, ApJ, 437, L75
Steidel, C. C., & Sargent, W. L. W. 1992, ApJS, 80, 1
Véron-Cetty, M.-P., & Véron, P. 1993, ESO Scientific Report No. 13
Wannier, P., & Wrixon, G. T. 1972, ApJ, 173, L119
Womble, D., Junkkarinen, V. T., & Burbidge, E. M. 1992, ApJ, 388, 55